PLOS | PATHOGENS

RESEARCH ARTICLE

Neutrophil-Derived MMP-8 Drives AMPK-Dependent Matrix Destruction in Human Pulmonary Tuberculosis

Catherine W. M. Ong[1,2], Paul T. Elkington[1,3], Sara Brilha[1], Cesar Ugarte-Gil[1,4], Maite T. Tome-Esteban[5], Liku B. Tezera[1,3], Przemyslaw J. Pabisiak[1], Rachel C. Moores[1], Tarangini Sathyamoorthy[1], Vimal Patel[5], Robert H. Gilman[6,7], Joanna C. Porter[8], Jon S. Friedland[1]*

1 Infectious Diseases and Immunity, Hammersmith Campus, Imperial College London, London, United Kingdom, **2** Division of Infectious Diseases, Department of Medicine, Yong Loo Lin School of Medicine, National University of Singapore, Singapore, **3** National Institute of Health Research (NIHR) Respiratory Biomedical Research Unit, Faculty of Medicine, University of Southampton, Southampton, United Kingdom, **4** Instituto de Medicina Tropical Alexander Von Humboldt, Universidad Peruana Cayetano Heredia, Lima, Peru, **5** The Heart Hospital, University College London Hospitals, London, United Kingdom, **6** Department of International Health, Johns Hopkins Bloomberg School of Public Health, Baltimore, Maryland, United States of America, **7** Asociación Benéfica Proyectos en Informatica, Salud, Medicina, y Agricultura (PRISMA), Universidad Peruana Cayetano Heredia, Lima, Peru, **8** Centre for Inflammation and Tissue Repair, Department of Medicine, University College London, London, United Kingdom

* j.friedland@imperial.ac.uk

Citation: Ong CWM, Elkington PT, Brilha S, Ugarte-Gil C, Tome-Esteban MT, Tezera LB, et al. (2015) Neutrophil-Derived MMP-8 Drives AMPK-Dependent Matrix Destruction in Human Pulmonary Tuberculosis. PLoS Pathog 11(5): e1004917. doi:10.1371/journal.ppat.1004917

Editor: Christopher M. Sassetti, University of Massachusetts, UNITED STATES

Received: December 12, 2015

Accepted: April 27, 2015

Published: May 21, 2015

Data Availability Statement: All relevant data are within the paper and its Supporting Information files.

Funding: CWMO is funded by the Singapore National Medical Research Council on an NRF-MOH Healthcare Research Scholarship. CUG was supported by the Wellcome Trust Master Fellowship of Tropical Medicine and Public Health (Grant 085777/Z/08/Z). RCM is a Wellcome Trust Clinical Research Fellow and TS an MRC Clinical Research Fellow. JSF and PE acknowledge support of the Biomedical Research Centre at Imperial College. JCP received support from Breathing Matters. The funders

Abstract

Pulmonary cavities, the hallmark of tuberculosis (TB), are characterized by high mycobacterial load and perpetuate the spread of *M*. *tuberculosis*. The mechanism of matrix destruction resulting in cavitation is not well defined. Neutrophils are emerging as key mediators of TB immunopathology and their influx are associated with poor outcomes. We investigated neutrophil-dependent mechanisms involved in TB-associated matrix destruction using a cellular model, a cohort of 108 patients, and in separate patient lung biopsies. Neutrophil-derived NF-kB-dependent matrix metalloproteinase-8 (MMP-8) secretion was up-regulated in TB and caused matrix destruction both *in vitro* and in respiratory samples of TB patients. Collagen destruction induced by TB infection was abolished by doxycycline, a licensed MMP inhibitor. Neutrophil extracellular traps (NETs) contain MMP-8 and are increased in samples from TB patients. Neutrophils lined the circumference of human pulmonary TB cavities and sputum MMP-8 concentrations reflected TB radiological and clinical disease severity. AMPK, a central regulator of catabolism, drove neutrophil MMP-8 secretion and neutrophils from AMPK-deficient patients secrete lower MMP-8 concentrations. AMPK-expressing neutrophils are present in human TB lung biopsies with phospho-AMPK detected in nuclei. These data demonstrate that neutrophil-derived MMP-8 has a key role in the immunopathology of TB and is a potential target for host-directed therapy in this infectious disease.

had no role in study design, data collection and analysis, decision to publish, or preparation of the manuscript.

Competing Interests: The authors have declared that no competing interests exist.

Author Summary

Neutrophil infiltration is characteristic of immune-induced pathology in tuberculosis but mechanisms whereby neutrophils cause tissue destruction are not fully understood. In this study, we show that neutrophils secrete the collagenase MMP-8 in response to direct infection with *Mycobacterium tuberculosis* and via cellular networks. MMP-8 is up-regulated in respiratory samples from TB patients, driving matrix destruction associated with neutrophil activation and reflects disease severity. Neutrophils are present adjacent to the wall of TB cavities in human histology specimens. The metabolic pathway AMP-activated protein kinase (AMPK) regulates neutrophil MMP-8 secretion with data supported by studies in human neutrophils from AMPK-deficient patients. Host-directed therapy against neutrophil MMP-8 may reduce innate-immune mediated tissue damage in TB.

Introduction

The lung cavity is a hallmark of pulmonary tuberculosis, a globally important disease of man. The cavity has high bacillary burden and is associated with spread of infection. Polymorphonuclear leukocytes or neutrophils are abundant in areas of TB lung cavities [1]. Excessive neutrophil recruitment associates with pathology in animal models [2, 3] and in man [4] but the mechanism of how neutrophils drive pathology in human TB is not defined.

Zinc-containing matrix metalloproteinases (MMPs) have key roles in the inflammatory immunopathology in a wide range of diseases including cancer and arthritis [5, 6]. On the basis of diverse evidence, it has been shown that a matrix-degrading phenotype develops in TB in which MMP activity is relatively unopposed by the specific tissue inhibitors of metalloproteinases (TIMPs) [7]. MMPs are crucial in granuloma formation in the zebrafish model of TB [8] and may drive different stages of lung pathology. Collagenases, a subgroup of the MMPs, are key in TB pathology since collagen is the main structural protein of the lung, the primary site of infection. Patients with pulmonary TB have increased collagenases which correlate significantly with radiological markers of tissue destruction [9, 10]. Neutrophils secrete MMP-8, a potent collagenase, and increased neutrophil-derived MMPs associate with disease severity in CNS-TB [11, 12], implicating neutrophils in the immunopathology of human TB.

The concept of metabolism regulating host immunity is only recently emerging [13]. Adenosine monophosphate-activated protein kinase (AMPK), a serine/threonine kinase is a central regulator of metabolic responses acting as an activator of cellular catabolism [13]. In addition, AMPK is known to have a role in immune responses determining the effector versus memory fate of CD8 T-cells [14]. Inhibition of glucose uptake and AMPK inhibition impedes T cell chemotaxis [15]. Dissecting the mechanism of how metabolism regulates immunity may be key to understanding immunity in chronic infections such as TB.

We hypothesize that neutrophils drive tissue destruction in human pulmonary TB. Animal models of infection such as murine strains which develop pulmonary necrosis and cavities are useful in dissecting areas of the immune response in TB [16–18]. Murine models also demonstrated the critical importance of IFN-γ and TNF-α in the host defence against TB [19–21]. However, there are inherent differences between murine and human neutrophils with divergences in cytokine secretion [22], peptides such as defensins [23], and intracellular signalling pathways [24]. Therefore, in this study, we investigate the role of the neutrophil in MMP-dependent tissue destruction in human pulmonary TB, a disease that affects man as the primary host, and examine the signaling pathways regulating this process.

First, we investigate the effect of neutrophil-derived collagenase MMP-8 in a human cellular model and examine MMP-8 expression and collagenolytic activity in patients. Neutrophils secrete MMP-8 on direct *M.tb* infection and in *M.tb*-infected monocyte-dependent networks. Neutrophil MMP-8 is expressed in TB patients' biopsy specimens, with the secretion of MMP-8 dependent on NF-kB. We found in a cohort of 108 TB patients and controls that increased MMP-8 is closely associated with neutrophil markers and correlates with radiological and clinical disease severity. Sputum MMP-8 from TB patients is functionally active, causing matrix destruction, and patients with pulmonary cavities on chest radiographs have higher MMP-8 concentrations in their respiratory secretions. Gelatin degradation in the respiratory samples is raised, but is not dependent on neutrophil gelatinase MMP-9. We demonstrate that AMPK regulates MMP-8 dependent tissue destruction, both at the level of protein secretion and gene expression, using data from a cellular model of infection and by investigating biopsy samples from TB patients and immune responses in AMPK deficient patients. Taken together, our data demonstrate that neutrophils cause tissue destruction in TB by an MMP-8-dependent process, regulated by the pro-catabolic AMPK pathway.

Results

Neutrophil MMP-8 is increased in TB and is expressed in neutrophils in patients with pulmonary TB

First, we investigated MMP-8 secretion from primary human neutrophils stimulated by live, virulent *M.tb*. Neutrophil MMP-8 secretion increased over time and in a dose-dependent manner in response to higher *M.tb* multiplicity of infection (MOI) (Fig 1A and 1B). TIMP-1 and -2 are the MMP inhibitors secreted by neutrophils [25, 26]. TIMP-1 was not secreted in response to stimulation by *M.tb* (S1A Fig). TIMP-2 concentrations increased significantly but to a 20-fold lower concentration than MMP-8 (S1B Fig). We demonstrated that neutrophil MMP-8 secretion was blocked by the NF-kB p65 subunit inhibitor Helenalin (IC_{50} 10–50 μM), in a dose-dependent manner and the effect was maximal at 100 μM (S1C Fig, $P<0.001$). The dose-dependent suppression of neutrophil MMP-8 was replicated with additional specific NF-kB inhibitors caffeic acid phenethyl ester (CAPE) [27] (S1D Fig) and SN50 [28] (S1E Fig). Neutrophil viability was greater than 95% for all conditions by FACS staining with Annexin V and live/dead dye (S2 Fig).

To determine the cellular source of MMP-8 in patients with TB, we analyzed lung biopsies from patients who were diagnosed with pulmonary TB. Polymorphonuclear neutrophils were observed along the entire circumference of the inner wall of cavities on H & E staining (Fig 1C). Neutrophil accumulation was confirmed by specific positive staining for neutrophil elastase (Fig 1D). Neutrophils in the same location stained positive for MMP-8 (Fig 1E and 1F). MMP-8 expression was also found in the central area of necrosis of granulomas (S3 Fig), suggesting that MMP-8 may be associated with the process of necrosis.

To determine if other proteases from neutrophils were similarly up-regulated, we analyzed MMP-9 (neutrophil gelatinase) secretion from *M.tb* infected neutrophils. *M.tb* caused a dose-dependent increase of MMP-9 secretion (Fig 1G). Furthermore, MMP-9 staining of patient lung biopsy specimens also showed presence of MMP-9 in neutrophils (Fig 1H).

M.tb infected and CoMTB-stimulated neutrophils degrade matrix

In addition to neutrophils, monocytes are among the early cells to be recruited in *M.tb* infection [29] and substantial cross-talk may occur between neutrophils and monocytes [30]. Using conditioned media from monocytes infected by *M.tb* (CoMTB) to model intercellular

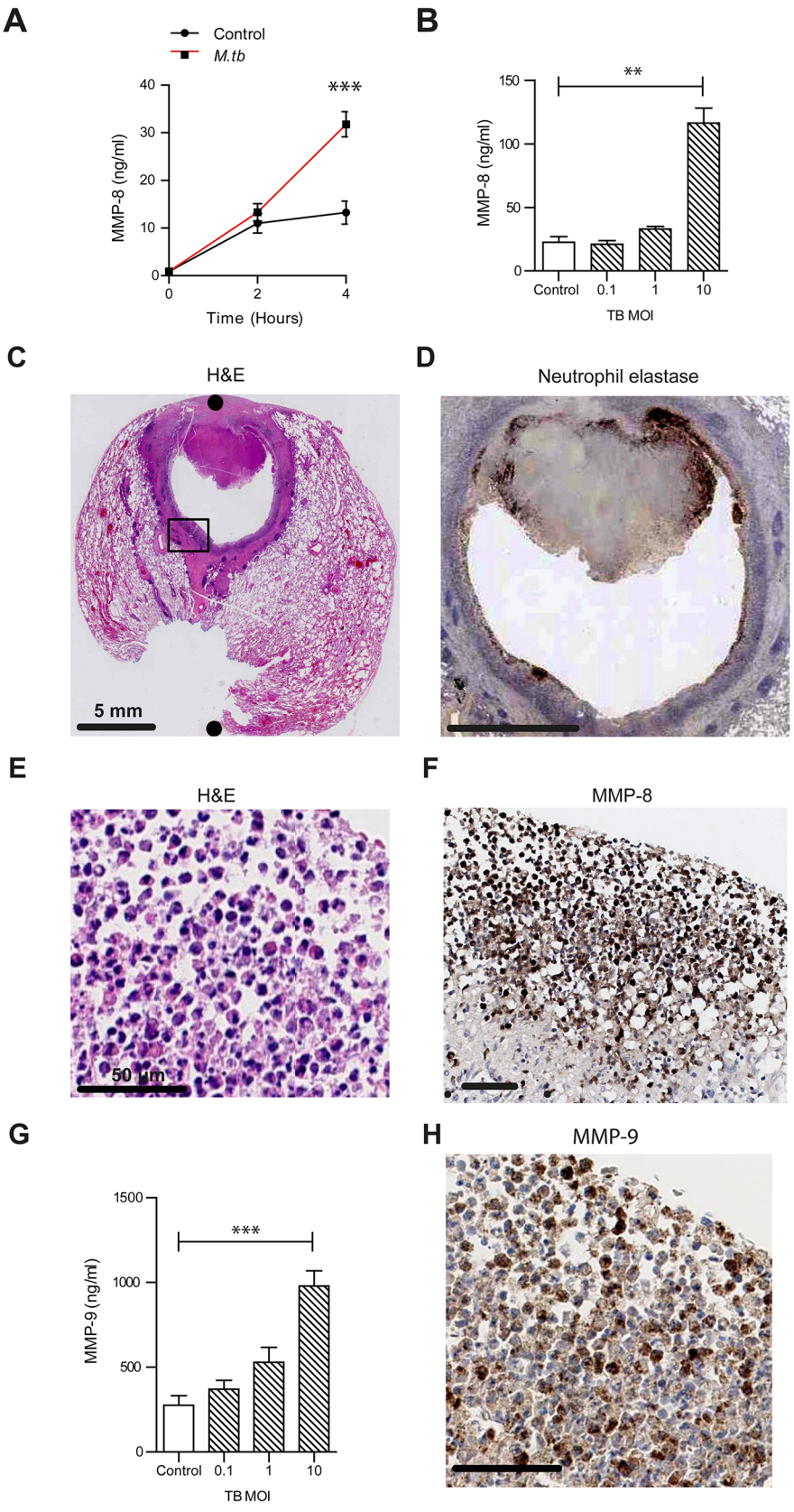
A
Control
M.tb
***
MMP-8 (ng/ml)
Time (Hours)
B
**
MMP-8 (ng/ml)
Control
0.1
1
10
TB MOI
C
H&E
5 mm
D
Neutrophil elastase
E
H&E
50 μm
F
MMP-8
G
***
MMP-9 (ng/ml)
Control
0.1
1
10
TB MOI
H
MMP-9

Fig 1. Neutrophil MMP-8 and -9 are upregulated in human TB. (**A**) Neutrophils were infected with *M.tb* MOI of 1. MMP-8 secretion was upregulated at 4h. (**B**) Increasing *M.tb* MOI caused greater neutrophil MMP-8, analyzed at 4h. Bars represent mean ± s.d. of experiments performed in triplicate and data are representative of a minimum of 2 independent experiments. (**C and D**) Human TB lung biopsy specimens stained with H&E and anti-neutrophil elastase shows neutrophil infiltration around the cavity wall. Both scale bars represent 5 mm. n = 5. (**E and F**) Magnified H&E and MMP-8 stains from Fig 1C inset shows neutrophils immunoreactive for MMP-8 around the cavity wall. Both scale bars represent 50 μm. (**G**) MMP-9 concentrations increase in a dose-dependent manner after *M.tb* infection at 4 hours. Bars represent mean ± s.d. of experiments performed in triplicate and data are representative of a minimum of 2 independent experiments. *** $P<0.001$ (**H**) Biopsy proven *M.tb* infected human lung specimens were stained for MMP-9 (inset from Fig 1C). Neutrophils were immunoreactive for MMP-9. Scale bar represents 50 μm. Statistical analysis was performed using two-way ANOVA with Bonferroni post-test or One-way ANOVA with Tukey's post-test. **$P<0.01$, ***$P<0.001$.

doi:10.1371/journal.ppat.1004917.g001

stimulation of neutrophils, we found significant up-regulation of MMP-8 secretion similar to *M.tb* infection (Fig 2A). We assessed the functional consequences of MMP-8 activity on degradation of Type I collagen, the main extracellular matrix fibril providing structural support in human lung parenchyma [31]. Both *M.tb*-infected and CoMTB-stimulated neutrophils degrade DQ collagen as assessed by a quantitative fluorescence assay (Fig 2B). Confocal microscopy demonstrated collagen degradation at the neutrophil-collagen interface both in *M.tb*-infected and CoMTB-stimulated neutrophils (Fig 2C and 2D). There was dose-dependent inhibition of collagenase activity to baseline when neutrophil supernatants were treated with doxycycline, an MMP inhibitor licensed in the USA for use in periodontal disease [32]. The effect was maximal after treatment with 100 μM doxycyline (Fig 2E, $P<0.001$).

Neutrophil MMP-8 is found on NETs

Next we showed that neutrophils generate NETs when stimulated with *M.tb in vitro* (S4A Fig), and NETs were digested by DNAse (S4B and S4C Fig). Neutrophil extracellular traps (NETs) are scaffolds containing DNA, histones and antimicrobial granule proteins. We demonstrated for the first time that MMP-8 co-localizes with NETs (Fig 3A and 3B). Next, we evaluated NETs in induced sputum from TB patients and healthy controls from a clinical study [33] (S1 Table). Sputum from TB patients had increased NET concentrations of 1548 mg/ml (± standard error 256 mg/ml) compared to controls at 372 mg/ml (± S.E. 150mg/ml) (Fig 3C, $P<0.001$). Citrulline H3, an established marker of NETs [34, 35] was detected in induced sputum of TB patients and not in healthy controls (Fig 3D). This was not due to dead or dying cells since these neutrophils do not contain citrulline H3 (S4D Fig).

MMP-8 in induced sputum of TB patients is closely associated with neutrophil markers and drives matrix degradation

MMP-8 is substantially elevated in the induced sputum of TB patients compared to other MMPs [33]. To determine if MMP-8 was neutrophil derived, we analyzed two established markers of neutrophil activation, myeloperoxidase (MPO) and neutrophil gelatinase associated lipocalin (NGAL) [36, 37] in induced sputum. In a cohort of 51 TB patients and 57 healthy controls randomly selected from our previously reported study of 137 patients [33], MPO and NGAL concentrations were increased in induced sputum of TB patients compared to controls (Fig 4A and 4B). Both sputum MPO and NGAL concentrations correlated strongly with MMP-8 ($r = 0.83$, $P<0.0001$ and $r = 0.68$, $P<0.0001$ respectively) (Fig 4C and 4D), indicating that MMP-8 in induced sputum of TB patients is likely to be principally derived from neutrophils.

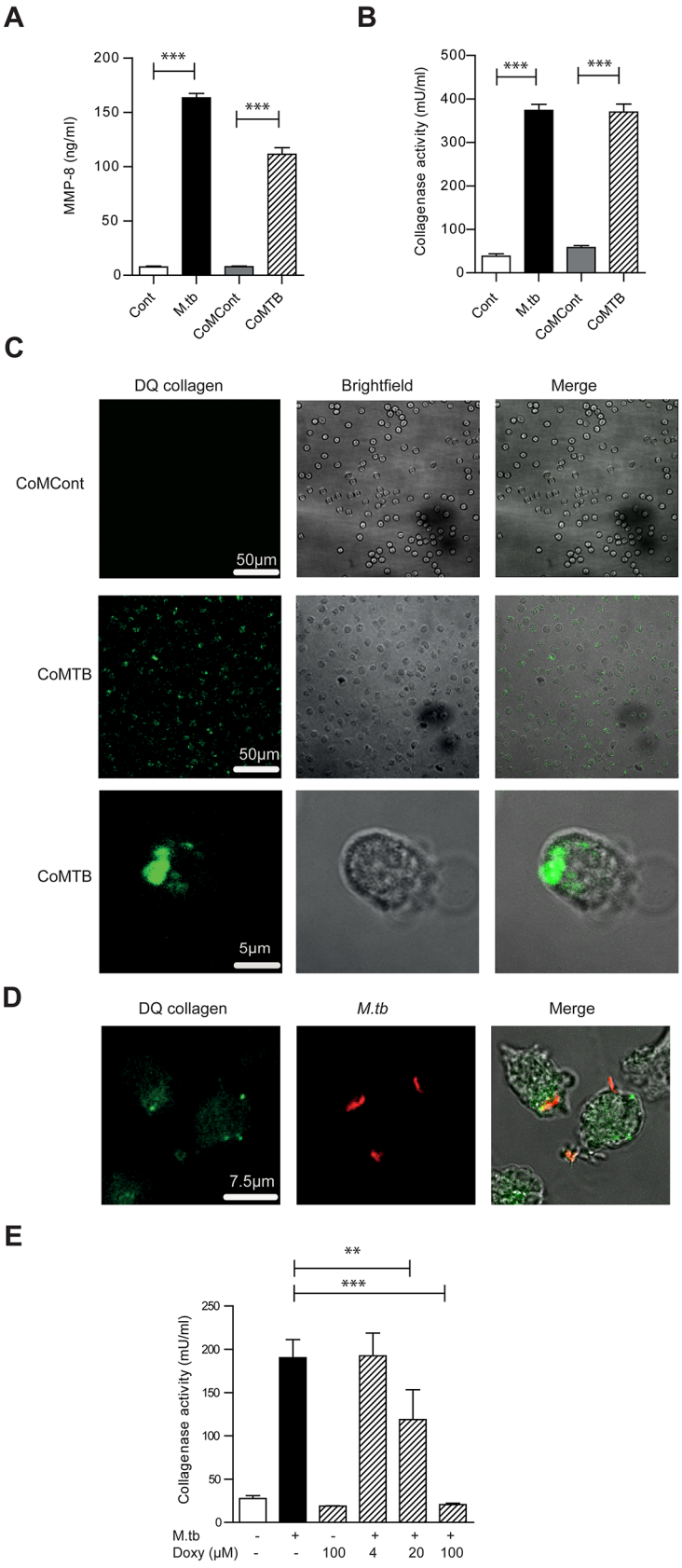
A
MMP-8 (ng/ml)
200
150
100
50
0
***
***
Cont
M.tb
CoMCont
CoMTB
B
Collagenase activity (mU/ml)
500
400
300
200
100
0
***
***
Cont
M.tb
CoMCont
CoMTB
C
DQ collagen
Brightfield
Merge
CoMCont
CoMTB
CoMTB
50µm
50µm
5µm
D
DQ collagen
M.tb
Merge
7.5µm
E
Collagenase activity (mU/ml)
250
200
150
100
50
0
**
***
M.tb - + - + + +
Doxy (µM) - - 100 4 20 100

Fig 2. *M.tb* and CoMTB-stimulated neutrophils degrade collagen. (**A**) Neutrophils were stimulated with either *M.tb* MOI of 10, CoMCont or CoMTB for 4 hours. *M.tb* and CoMTB up-regulated MMP-8 secretion analyzed by ELISA. (**B**) Cell-free supernatants from (A) were incubated with Type I DQ collagen. Bars represent mean ± s.d. of experiments performed in triplicate and are representative of a minimum of 2 independent experiments. (**C**) CoMTB caused increased collagen breakdown by neutrophils, resulting in greater fluorescence of DQ collagen. (**D**) Neutrophils were infected with *M.tb* MOI 10, fixed and *M.tb* stained with *anti-M.tb* Ab. Infected cells degraded DQ collagen, increasing fluorescence. (**E**) Cell-free supernatants from neutrophils infected with *M.tb* at MOI 10 were added with doxycyline to Type I DQ collagen. Doxycycline suppressed collagenase activity in a dose-responsive manner. Bars represent mean ± s.d of an experiment performed in biological triplicates and represents 2–3 independent experiments. Analysis performed using One-way ANOVA with Tukey's post-test. ** $P<0.01$, ***$P<0.001$.

doi:10.1371/journal.ppat.1004917.g002

Next, we demonstrated that induced sputum from TB patients had increased collagenase activity compared to healthy controls using the DQ collagen degradation assay (Fig 4E, $P = 0.02$), confirmed on confocal microscopy (Fig 4F). Sputum MMP-8 concentrations strongly correlated with collagenase activity (r = 0.7, $P = 0.0004$) (Fig 4G) and MMP-8 neutralization decreased collagenase activity in respiratory secretions of TB patients ($P = 0.01$) (Fig 4H). When the cohort was stratified according to the presence or absence of lung cavities, patients with pulmonary cavitation secreted a median of 5-fold higher MMP-8 concentration than those without cavities. ($P<0.028$, Fig 4I). In addition, MMP-8 sputum concentrations positively correlated with the TB score (r = 0.56 for n = 108; $P<0.0001$), a clinical marker of disease severity. The other major neutrophil-derived MMP, MMP-9, had a much weaker although statistically significant correlation with TB score (r = 0.3453 for n = 108; $P = 0.003$). Analyzing CXR consolidation score as a radiological marker of tissue destruction demonstrated a similar strong MMP-8 correlation (r = 0.52 for n = 74; $P<0.0001$) and a weaker MMP-9 correlation with pathology (r = 0.31 for n = 74; $P = 0.0077$).

To determine if MMP-9 contributes to matrix destruction in TB patients, we assessed the gelatinase activity of the respiratory secretions. Induced sputum from TB patients showed an increased gelatinase activity ($P<0.0001$; S5A Fig). However, MMP-9 neutralization with an inhibitory antibody at 10 μg/ml which completely suppresses gelatinase activity from MMP-9 [38], did not decrease gelatinase activity in the respiratory secretions (S5B Fig).

AMP-activated protein kinase regulates neutrophil MMP-8 secretion in TB in vitro

To investigate the key regulatory pathways of neutrophil MMP-8 secretion, we performed a screening human phosphokinase array and observed that the AMP-activated protein kinase (AMPK) pathway was consistently activated in *M.tb*-infected neutrophils, especially AMPKα2 (T172) (Fig 5A). This activation was confirmed by immunoblotting (Fig 5B). Components of the MAP-kinase, STAT pathways, p53 and Src family of kinases were also activated consistent with previous data [39–41] (S6A, S6B and S6C Fig). AMPK is considered a master regulator of cellular energy homeostasis, existing as a heterotrimeric complex comprising catalytic α-subunits and regulatory β- and γ-subunits [13]. Its activation sets off a cascade of catabolic pathways including glycolysis and ketogenesis which can lead to the wasting which is characteristic in TB patients. We demonstrated that AMPKα was activated by phosphorylation in neutrophils directly infected with *M.tb* (Fig 5C).

The specific AMPK inhibitor Compound C (Comp C) blocked neutrophil MMP-8 secretion in a dose-dependent manner towards baseline levels (Fig 5D) and also suppressed gene expression of neutrophil MMP-8 (Fig 5E), confirming AMPK is functionally active in regulating neutrophil MMP-8 secretion. Since the AMPK pathway may be downstream of the Akt/PI3-kinase pathway [42, 43] and the Akt/PI3-kinase pathway may drive tissue destruction in TB [44], we

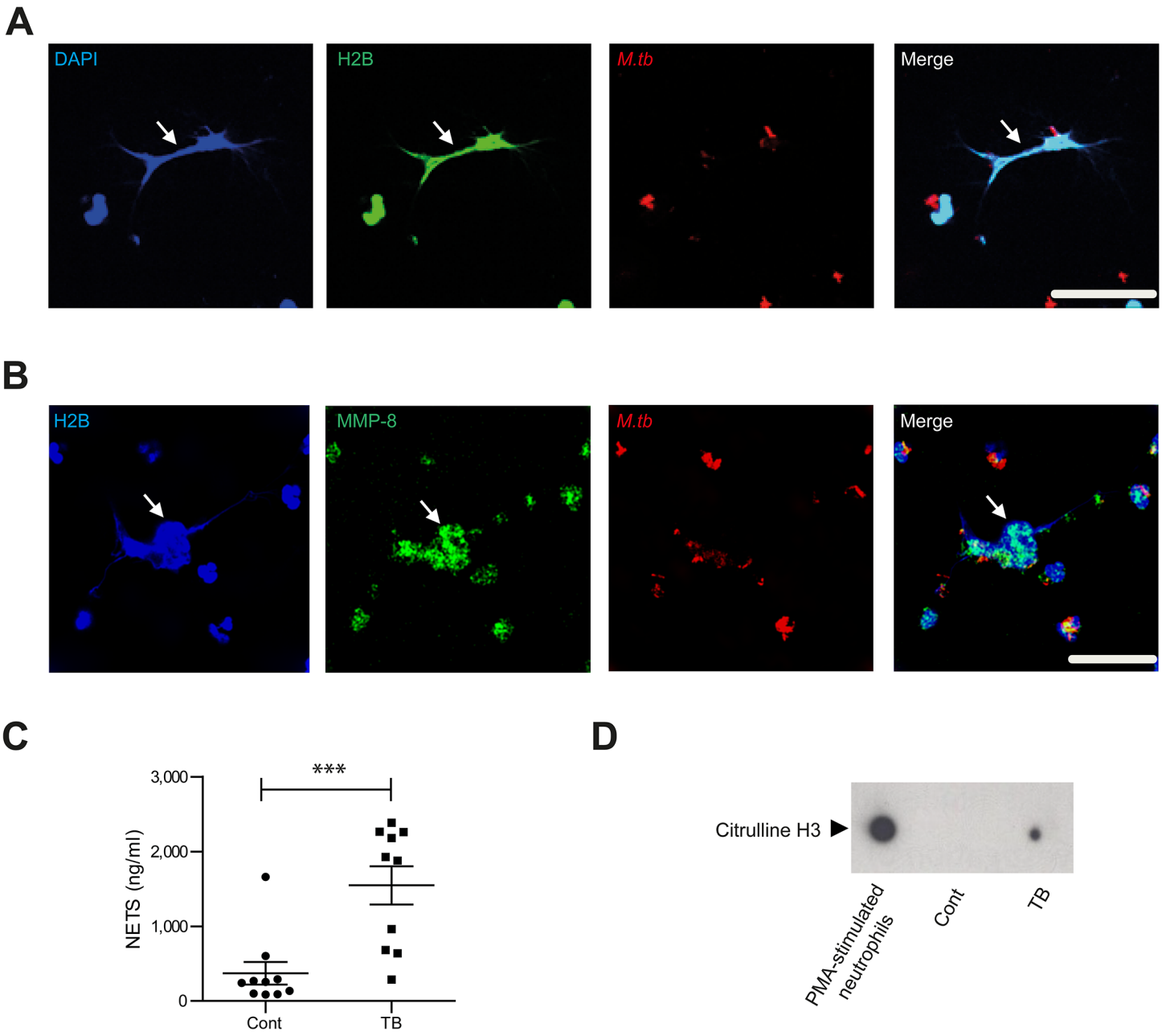

Fig 3. Neurophil MMP-8 associates with NETs. (**A** and **B**) Neutrophils were infected with *M.tb* MOI of 10 for 4 hours and NETs stained with DAPI (blue), anti-histone 2B (H2B, green) or anti-MMP-8 (green), while *M.tb* was stained with anti-*M.tb* Ab (red). *Mtb* induces NET formation which do not adhere to the shape of the neutrophil nuclei (White arrows). Scale bars represent 25 μm. (**C**) Induced sputum NETs were greater in patients with TB than healthy controls ($n = 10$ both groups analyzed by Student's t-test). (**D**) NETs marker citrulline H3 is present in induced sputum of TB patients but not in healthy controls. Blot representative of $n = 2$ both groups.

doi:10.1371/journal.ppat.1004917.g003

investigated whether this path regulates human neutrophil MMP-8 secretion. Neutrophil Akt was phosphorylated in response to CoMTB (S7A Fig) but MMP-8 secretion was not suppressed by either the Akt-inhibitor (Akt-i) or the broad-spectrum PI3-kinase inhibitor LY 294002 (S7B and S7C Fig). We also examined whether the mTOR/p70S6 kinase regulated neutrophil MMP-8 secretion as this is downstream of AMPK [45]. p70S6 kinase was phosphorylated in neutrophils stimulated by CoMTB (S7D Fig) but the mTOR inhibitor rapamycin did not

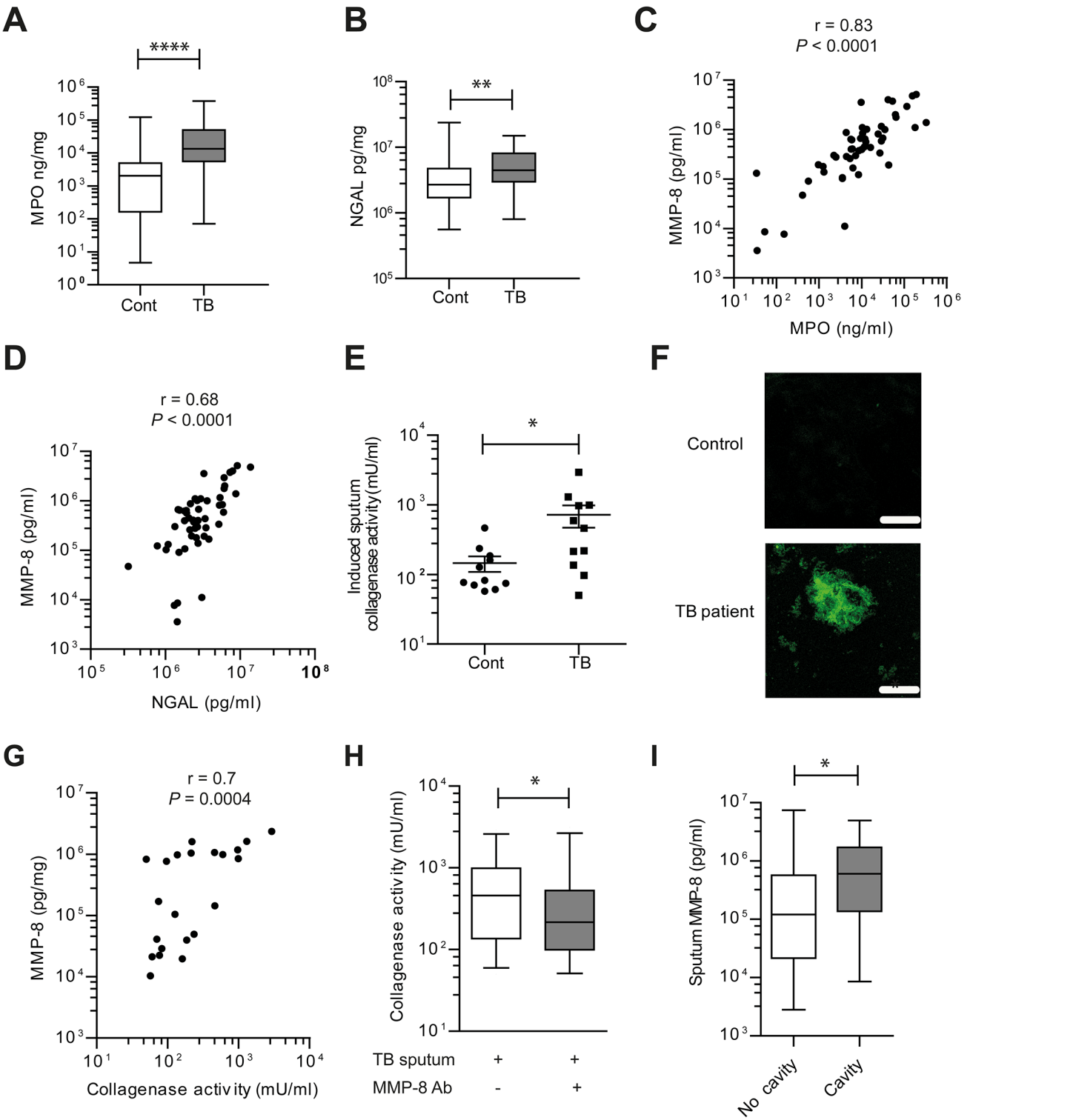

Fig 4. Induced sputum samples of pulmonary TB patients have increased collagenase activity due to neutrophil-derived MMP-8. (**A and B**) Induced sputum MPO and NGAL was analyzed by ELISA from $n = 51$ TB patients and $n = 57$ healthy controls. MPO and NGAL were increased in patients with pulmonary TB. (**C and D**) Induced sputum MMP-8 closely correlated with both MPO and NGAL in TB patients, performed using Spearman's correlation coefficient. (**E**) Induced sputum collagenase activity is increased in TB patients. ($n = 11$ each group). Subsets analyzed were representative of the whole cohort analyzed by Mann-Whitney test. (**F**) Confocal microscopy shows increased DQ collagen degradation in induced sputum of TB patient relative to control. Image is representative of $n = 3$ each group. Scale bars represent 50μm. (**G**) Induced sputum MMP-8 and collagenase activity correlate, analyzed by Spearman's correlation coefficient ($n = 22$). (**H**) MMP-8 neutralization suppresses induced sputum collagenase activity from TB patients. MMP-8 neutralizing

antibody was added to activated induced sputum with Type I DQ collagen ($n = 11$). Box and whiskers represent 10–90th percentile with comparison using Wilcoxon-Sign rank test. (**I**) Induced sputum MMP-8 were higher in patients with pulmonary cavities than those without. * $P< 0.05$, ** $P<0.01$, **** $P<0.0001$.

doi:10.1371/journal.ppat.1004917.g004

inhibit neutrophil MMP-8 secretion (S7E Fig), indicating that neutrophil MMP-8 secretion is independent of this pathway.

AMPK regulates neutrophil MMP-8 secretion in TB in patients

Finally, we studied AMPK *in vivo*. In human TB lung specimens, AMPKα was phosphorylated within the nuclei of neutrophils in TB cavities (Fig 6A and 6B), indicating a state of energy depletion [46]. AMPK regulation of neutrophil MMP-8 was further investigated using neutrophils from a group of patients with defects in AMPK activation. Their clinical phenotype is typically similar to those found in glycogen storage disorders [47]. Genotypically, these patients

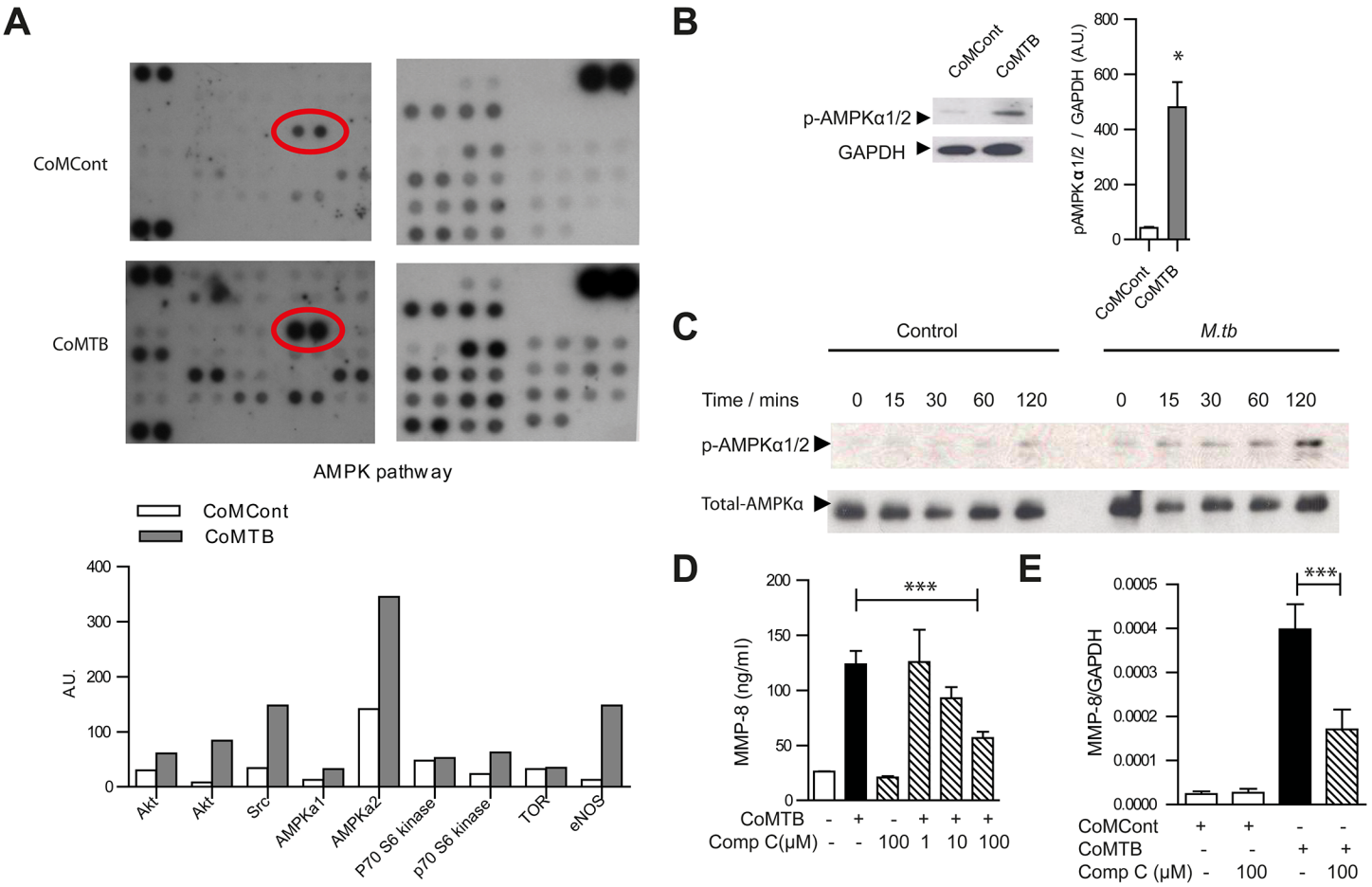

Fig 5. AMPK regulates neutrophil MMP-8 secretion in TB *in vitro*. (**A**) Human phosphokinase array. Neutrophils were stimulated with CoMCont or CoMTB. Representative blot from $n = 4$ healthy donors. Red circle highlights increased AMPKα2 phosphorylation in CoMTB-stimulated cells, with densitometric analysis of components of AMPK pathway below. (**B**) CoMTB stimulation phosphorylates AMPKα1/2 analyzed by western blotting and gel densitometry. Neutrophils were stimulated for 30 minutes. Bars represent mean ± s.e.m from $n = 3$ donors. (**C**) Neutrophils were infected with *M.tb* MOI of 10 and cell lysates immunoblotted for phospho-AMPKα (T172) at defined time points. *M.tb* caused maximal phosphorylation at 120 mins. (**D**) Compound C (Comp C) pre-incubation for 30 minutes before CoMTB stimulation suppresses neutrophil MMP-8 secretion at 4 hours. (**E**) Compound C (Comp C) was pre-incubated for 30 minutes before stimulation with CoMCont or CoMTB for 24 hours with MMP-8 gene expression analyzed by real-time PCR normalized to GAPDH. Bars represent mean ± s.d. of an experiment performed in biological triplicates on at least 2 occasions. *$P<0.05$, ***$P<0.001$. Analysis was performed using one-way ANOVA with Tukey's post-test.

doi:10.1371/journal.ppat.1004917.g005

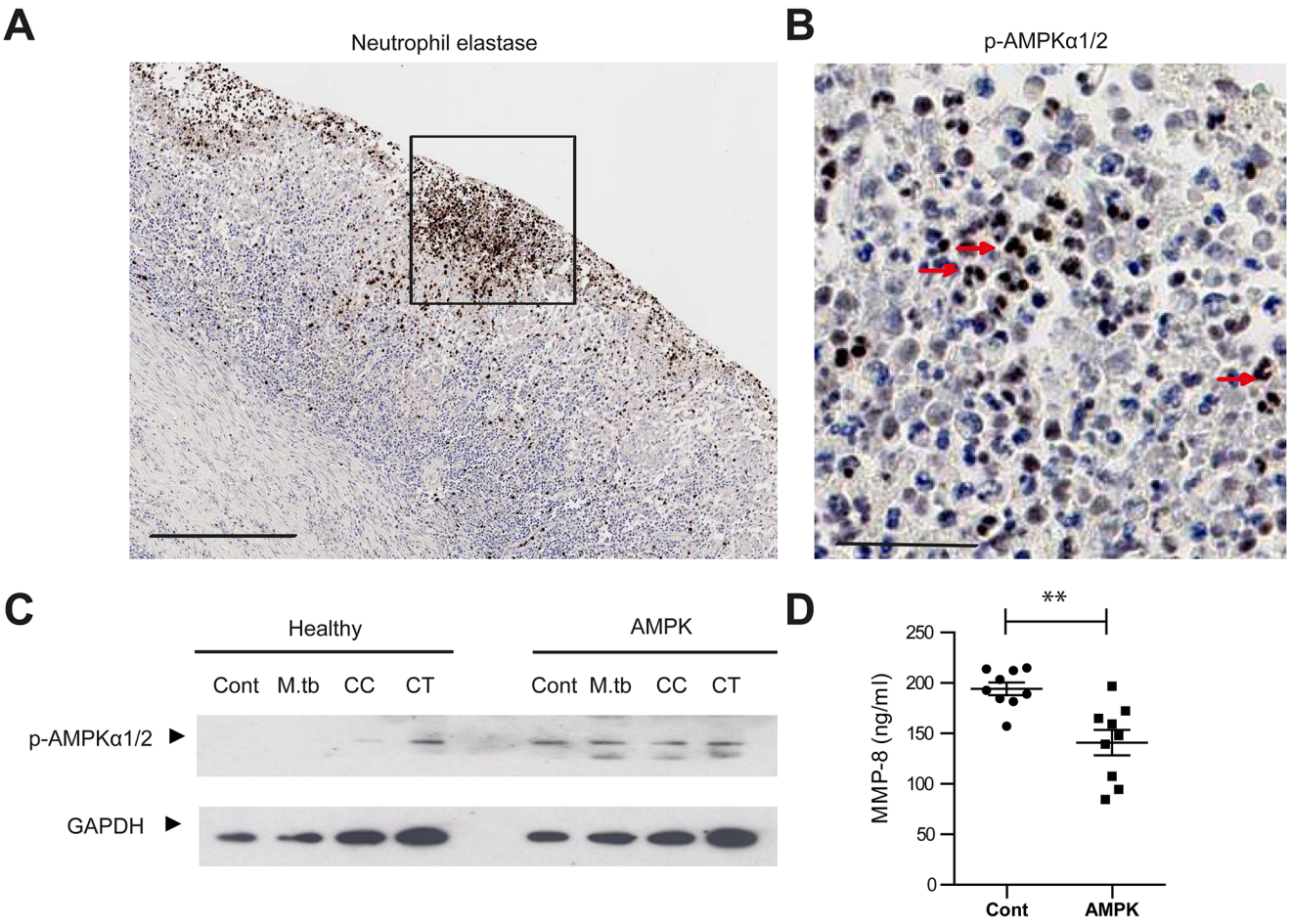

Fig 6. AMPK regulates neutrophil MMP-8 secretion in patients. (**A**) Neutrophils are present in human TB lung cavity wall and stain positive for neutrophil elastase. Scale bar 250μm. (**B**) Neutrophils express phospho-AMPKα (T172) in the nuclei (red arrows) (inset of A). Scale bar 50μm. (**C**) Neutrophils from healthy donors and patients with AMPK deficiency were stimulated with *M.tb* MOI of 10, CoMCont or CoMTB for 30 minutes. In patients, AMPK is constitutively phosphorylated, resulting in a functional deficiency. Blot representative of 6 healthy controls and AMPK patients. (**D**) Neutrophils from healthy donors and patients with AMPK deficiency were stimulated with CoMTB. $n = 3$ both groups. Neutrophils derived from AMPK patients secreted less MMP-8 when stimulated than cells from healthy donors. Experiments were performed in biological triplicates and each point represents a sample. Analysis was performed using one-way ANOVA or two-tailed t-test. ** $P<0.01$, ***$P<0.001$.

doi:10.1371/journal.ppat.1004917.g006

have an AMPKγ2 mutation [48]. AMPKα mutations have not been described in man. In these patients, AMPKα was phosphorylated in both unstimulated and stimulated neutrophils but not in healthy donors, demonstrating increased basal phosphorylation of AMPKα (Fig 6C). Such increased basal AMPK activity reduces the sensitivity of the protein kinase to AMP, resulting in functional AMPK deficiency [47]. MMP-8 secretion from AMPK-deficient neutrophils stimulated by CoMTB was significantly less than MMP-8 secreted by AMPK-replete neutrophils (Fig 6D, $P<0.01$), implicating AMPK in the regulation of neutrophil MMP-8 secretion in man.

Discussion

Neutrophils are emerging as key mediators of TB-associated inflammation. They drive the unique TB transcript signatures in man [39] and predominate in respiratory secretions of patients with pulmonary TB [1, 49]. We found sputum from TB patients had increased MMP-8 concentrations, neutrophil myeloperoxidase (MPO) and neutrophil gelatinase associated

lipocalin (NGAL) compared to controls. MMP-8 was strongly associated with markers of neutrophil activation, MPO and NGAL, indicating that sputum MMP-8 is likely to be neutrophil-derived. Neutrophils expressing MMP-8 were found in the inner walls of tuberculous cavities and may further erode the lung matrix, extending previous findings that neutrophils are the predominant phagocytic cells in the respiratory secretions of TB patients [1]. We also found higher MMP-8 in TB patients with cavities on their chest radiographs than those without cavitation. These findings are consistent with and extend our previous data in smaller groups of patients that demonstrated a trend to increased MMP-8 compared to patients with respiratory symptoms [9, 10]. Furthermore, MMP-8 is significantly elevated in plasma samples of patients with TB compared to respiratory symptomatics [50]. These observations underscore the importance of collagenases, such as MMP-8 and MMP-1, which are the only enzymes capable of degrading the collagen triple helix at neutral pH. The consistent elevation of MMP-8 across the different patient cohorts implicates neutrophils as key players in tissue destruction in TB.

In animal models of TB, neutrophil influx is associated with poorer outcomes with higher bacterial burden, earlier mortality and tissue inflammation [51–53]. However, the mechanisms linking neutrophil excess and poor outcomes are unclear. In our human study, *M.tb* drove neutrophil MMP-8 secretion, causing destruction of collagen, the main structural protein in human lung, both *in vitro* and in TB patients. We showed neutrophil MMP-8 closely correlated with sputum collagenase activity as well as clinical CXR score and TB severity score, implicating neutrophils in driving pathology in man by their collagenolytic activity. MMP-8 was also associated with NETs in *M.tb* infection and NET components such as citrulline H3, which were not present in dead neutrophils, were increased in the respiratory secretions of TB patients. This may further contribute to immunopathology since NETs are recognized to induce cell death [54, 55]. It is likely that different MMPs predominate in different stages of disease in TB immunopathology. There is good evidence that neutrophils are present not only during the acute phases of TB infection with macrophages, but are also a dominant cell type at the site of established infection of the cavity together with lymphocytes [1, 51, 52]. Such neutrophils contain high concentration of pre-synthesized MMP-8 [56], and so can drive the later stages of TB which leads to lung cavitation, morbidity and death

MMP-8 inhibition may be a target to abrogate excessive host tissue destruction. MMP-8 is a critical mediator of lung parenchymal damage other lung diseases, such as COPD [57] and ventilator-induced lung injury, and MMP-8 inhibition improves outcomes in a murine model of lung injury [58]. We showed higher MMP-8 in the respiratory secretions of patients with cavities than those without and MMP-8 neutralization decreased the matrix destruction in the sputum of TB patients. Although neutrophil gelatinase MMP-9 is secreted in TB and expressed in TB patients, neutralizing MMP-9 did not reduce gelatinase activity in TB patients. Neutrophil MMP-8 secretion in TB was inhibited by NF-kB inhibitors helenalin, CAPE and SN50 without altering neutrophil viability. Furthermore, doxycycline reduced neutrophil collagenase activity to baseline and MMP-8 neutralizing antibody decreased collagen destruction *ex vivo* in TB patients. Such immunomodulatory agents have potential to reduce tissue destruction in TB.

For the first time in TB, we have shown that there is interaction between the metabolic AMPK signaling pathway in the regulation of neutrophil MMP-8 secretion and innate-immune mediated tissue destruction. AMPK activates catabolic pathways such as fatty acid oxidation and glycolysis to generate ATP, while switching off energy-consuming processes including protein and fatty-acid biosynthesis and cell-cycle progression. Two studies have shown that the development of lung injury in murine models is dependent on the pro-catabolic AMPK pathway [59, 60] with AMPK activation decreasing lung injury. This contrasted with our findings

where AMPK inhibition decreased neutrophil MMP-8 secretion, and maybe due to AMPK having divergent effects on different cells.

The AMPK pathway was up-regulated in our cellular model and drives neutrophil MMP-8 secretion and gene expression, which was inhibited by the AMPK inhibitor Compound C. This finding was repeated in a small cohort of extremely rare patients with functional AMPK deficiency from a γ_2-subunit mutation, where *M.tb*-driven neutrophil MMP-8 was decreased compared to healthy volunteers. While this does not definitively prove that AMPK regulates MMP-8 secretion as metabolic differences in neutrophils may cause divergent secretion, it implicates AMPK in driving neutrophil-mediated pathology by MMPs in TB. This finding is in keeping with a recent study where AMPKα2 deficient mice had decreased MMP-2 and were found to be resistant to developing abdominal aneurysms, a process which was demonstrated to be MMP-dependent [61]. Recent data demonstrate that AMPK has the ability to shuttle through the nucleus and contains both cytosolic components and nuclear components [46] with the ability to control transcription [62]. We showed AMPKα was phosphorylated in *M.tb*-infected neutrophils and adjacent to human TB lung cavities, with phospho-AMPKα located in the nuclei, signifying a state of energy depletion [46].

Together, our data from our human cellular model and in patients demonstrate that neutrophils drive MMP-8-dependent tissue destruction in TB, providing an insight as to how excessive neutrophil infiltration exerts a detrimental effect on the host. This process is controlled by the metabolic regulator AMPK as demonstrated *in vitro* and in AMPK deficient patients. This study highlights a previously unappreciated connection between metabolic paths that directly interact with innate immune responses causing immunopathology in human TB. Interventions specifically targeting the intersection of metabolic and innate immune responses to decrease tissue destruction may improve outcomes in TB and other inflammatory disorders.

Materials and Methods

Reagents and antibodies

Mouse anti-human beta-actin, rapamycin and doxycycline hyclate were from Sigma. Helenalin, SN50 and Compound C were from Merck Biochemicals. Caffeic acid phenethyl ester (CAPE) was from Tocris (R&D Biosystems). Mouse anti-human MMP-8, mouse anti-human MMP-9, rabbit anti-human GAPDH, rabbit anti-human histone 2B, rabbit anti-human phospho-p70S6k (T229), rabbit anti-Mycobacterium tuberculosis, rabbit anti-human neutrophil elastase, rabbit anti-human phospho-AMPK alpha 1 and 2 (T172), sheep anti-human histone 2B, rabbit anti-human histone H3 (citrulline 2 + 8 + 17), donkey anti-Sheep IgG DyLight 488, goat anti-mouse DyLight 549, goat anti-rabbit IgG Cy5 were from Abcam. Rabbit anti-human phospho-Akt, total-Akt, phospho-AMPKα1/2 (T172), total AMPKα, and goat anti-rabbit HRP linked were from Cell Signalling Technology. Goat anti-mouse IgG (H+L) was from Jackson Immunoresearch laboratories. Goat anti-human MMP-8 was from R&D Biosystems and mouse anti-human MMP-9 was from Millipore. Rabbit anti-human MMP-8 was from Novus Biologicals. Mouse anti-human neutrophil elastase was from Dako. Mouse anti-human MMP-9 was from Millipore.

Recruitment of patients and controls

Ethics statement. For recruitment of TB patients and controls, the Institutional Review Board from Universidad Peruana Cayetano Heredia and Direccion de Salud Lima Este (Lima, Peru) approved this study and written informed consent was obtained from all participants. For AMPK patients, the study received the Institutional Review Board approval from Central London Research Ethics Committee and written informed consent was obtained from all

patients. For extraction of primary human neutrophils, ethical approval for obtaining healthy human volunteer blood was provided by the Outer West London Research Ethics Committee and written informed consent was obtained from individuals. Ethical consent for the study of anonymized paraffin-embedded sections from histopathology was obtained from the Hammersmith Hospitals Research Ethics Committee in accordance with The Human Tissue Act 2004 and written informed consent was obtained from subjects who donated their biopsy specimens.

TB patients and controls. A subset of 51 TB and 57 control patients were analysed from the original cohort of 137[33]. In brief, TB patients were recruited prior to starting TB therapy and were microbiologically positive, aged over 18 years, had no prior history of TB or TB treatment and were HIV negative. Healthy controls aged over 18 years had no symptoms associated with TB, a normal chest radiograph and negative sputum TB culture. Induced sputum samples of at least 3 mls was obtained from TB patients and healthy controls and were sterile filtered using a 0.2μm Durapore membrane (Millipore). Total protein concentrations were measured using Bradford assay (Bio-Rad). Disease severity was assessed using an established clinical TB Score [63]. This is a clinical score that evaluated the following: cough, hemoptysis, dyspnea, chest pain, night sweats, conjunctival pallor, tachycardia, axillary temperature above 37°C, body mass index and middle upper arm circumference (MUAC) with a total possible score of 13. Chest radiographs were scored for extent of pulmonary consolidation with Image J 1.43U (NIH, USA) using the formula: (Area of TB consolidation/Total lung area) x (Mean absorbance of TB consolidation/Mean lung absorbance) x 100% as before [33].

AMPK patients and controls. The cardiology specialty consultation service of The Heart Hospital, University College London identified patients with cardiomyopathy, who were confirmed on genotyping to have an AMPKγ2 mutation. Neutrophil isolation was performed concurrently from each patient and from a healthy control with cells stimulated concurrently.

M.tb culture

M. tuberculosis H37Rv was cultured in supplemented Middlebrook 7H9 medium (BD Biosciences). For infection experiments, mycobacteria were used at mid-logarithmic growth at an optical density of 0.60 (Biowave cell density meter; WPA).

Cell culture and stimulation

Whole blood were drawn in preservative-free heparin and mixed with equal volumes of 3% dextran saline to remove erythrocytes. Neutrophils were isolated from the resulting cell suspension using Ficoll-Paque density centrifugation and three rounds of hypotonic lysis. Neutrophil purity was over 95% by FACS and viability >99% by trypan blue assay. In some experiments, neutrophils were pre-incubated with specific inhibitors/agents as indicated for 30 minutes unless otherwise stated. In all experiments involving live *M. tuberculosis* H37Rv, tissue culture medium was sterile filtered through 0.2 -μm Anopore membranes (Millipore) before removing from the CL3 laboratory. All experiments were performed using 4 hour incubations unless otherwise stated.

Primary human blood monocytes were prepared from donor leukocyte cones from healthy donors (National Blood Transfusion Service, UK). After density gradient centrifugation (Ficoll Paque) followed by adhesion purification, monocyte purity was over 95% by FACS analysis. Monocytes were infected with *M.tuberculosis* at a multiplicity of infection (MOI) of 1. After incubation at 37°C for 24 h, conditioned medium was harvested and was termed CoMTB. Media from uninfected monocytes was termed CoMCont.

ELISAs for TIMP-1/2, MPO and NGAL

TIMP-1 and 2 concentrations were measured using the Duoset ELISA Development System (R&D Systems) and detected a minimum of 31.2 pg/ml for both. The human MPO Quantikine ELISA kit (R&D Systems) was performed according to manufacturer's instructions and the lower limit for MPO detection was 0.1 ng/ml. NGAL was measured using the human NGAL ELISA kit (Bioporto Diagnostics) which had minimum detection limit of 1.6 pg/ml.

Luminex array

MMP-8 and -9 concentrations were analyzed by Fluorokine multianalyte profiling kit according to the manufacturer's protocol (R&D Systems) on the Luminex platform (Bio-Rad). The minimum level of detection for MMP-8 and -9 was 110 pg/ml and 65 pg/ml respectively. Cytokine concentrations were analyzed using a human 30-plex panel (Invitrogen).

Human phosphokinase array

The Proteome Profiler Human Phospho-kinase array kit (R&D Systems) which detects 45 phosphorylated proteins was performed according to the manufacturer's protocol and developed with the ECL system (Amersham Biosciences). Thirty minutes after neutrophils were stimulated with CoMTB, the cells were pelleted and lysed in lysis buffer. Equal amounts of total protein were loaded on to each array. Densitometric analysis of arrays was performed using Scion Image version Beta.4.0.2.

DQ collagen and gelatin degradation assays

Type I collagen and gelatin degradation was assessed using the EnzChek Gelatinase/Collagenase Assay kits (Molecular Probes). Samples were activated with 2 mM of 4-amino-phenyl mercuric acetate (APMA) for 1 hour at 37°C. 80μL of reaction buffer or inhibitor (doxycyline hyclate, Goat anti-human MMP-8 or Mouse anti-human MMP-9) were added with 20μL of either DQ collagen or gelatin (Invitrogen) at a final concentration of 25μg/ml. Activated samples were subsequently added, and activity detected at specified times using a fluorometer (FLUOstar Galaxy).

Isolation and quantification of neutrophil extracellular traps (NETs)

Human neutrophils were infected with *M.tb* at an MOI of 10 and 20 nM PMA was used as a positive control. 5 U/ml of micrococcal nuclease (Fermentas) was added in each well for 10 minutes at 37°C, after which EDTA was used to halt the reaction. Supernatants were collected, sterile filtered and stored at 4°C. NETs were quantified using QuantiT PicoGreen (Invitrogen) according to manufacturer's instructions.

Immunoblotting

Pelleted neutrophils infected with *M.tb* or stimulated with CoMTB were mixed with SDS lysis buffer. Samples were run on the NuPAGE 4–12% Bis-Tris gels with SDS Running buffer (Invitrogen). Protein was transferred onto a nitrocellulose membrane (GE Healthcare). Primary antibody was diluted in 5% BSA/0.1% Tween and incubated overnight at 4°C with agitation. Secondary antibody was added diluted in blocking buffer. Luminescence was demonstrated with ECL Substrate Reagent (Amersham Science) according to manufacturer's instructions and exposing the membrane to Hyperfilm ECL. Densitometric analysis was performed using Image J 1.43U (NIH, USA).

Real-time PCR

Total RNA was extracted from 2 x 10^6 neutrophils using the RNeasy Mini Kit (Qiagen). Quantitative real-time RT-PCR was performed using the OneStep RT- PCR master mix (Qiagen) according to the manufacturer's instruction on a Stratagene Mx3000P platform using 5–10 μg per sample. MMP-8 primer and probe mixes were obtained from Applied Biosystems. GAPDH (Forward primer 5'- CGCTTCGCTCTCTGCTCCT-3', reverse primer 5'- CGAC CAAATCCGTTGACTCC-3', probe 5'-HEX-CGTCGCCAGCCGAGCCACAT-TAMRA-3') was analyzed in parallel. To accurately determine the quantitative change in RNA, standard curves were prepared from plasmids subjected to real-time PCR as above. MMP-8 data were normalized to GAPDH detected in the same sample.

Flow cytometry

Cell viability was assessed by staining neutrophils with Annexin V-FITC apoptosis detection kit (eBioscience, Affymetrix, California, USA) and live/dead fixable dead cell stain kit (Invitrogen). Neutrophils were stimulated with 200 ng/ml staurosporine to induce apoptosis and this was used as a positive control for all experiments. Annexin V was detected on the FL-1 channel and live/dead dye on FL-3. A total of 50,000 events were gated and analysed on BD FACSCalibur flow cytometer using CellQuest. Data was analysed using FlowJo 7.6.5 (Tree Star).

Immunofluorescence microscopy

Permanox chamber slides (Nunc Labtech) were coated with 0.1 mg/ml fibrinogen with or without 25 μg/ml of DQ collagen for 30 minutes. For experiments involving NETs, 10 Ü/ml DNase (Fermentas) was added for 20 minutes at room temperature at the end of the experiment. Samples were then fixed with 4% paraformaldehyde for 30 minutes and permeabilized with 0.5% saponin for 10 minutes. Cells were washed before blocking with 10% human AB serum with 2.5% BSA and 0.05% saponin. Primary antibodies were added overnight. Chamber slides were washed prior to the addition of secondary antibodies. The chambers were subsequently removed from the slide, and Fluoroshield Mouting medium with DAPI (Abcam) was added. Images were captured using Leica confocal microscope (Leica TCS SP5) and processed using Leica LAS AF Lite 2.6.0 (Leica Microsystems, Germany) and Image J 1.43U (NIH, USA).

Immunohistochemistry

Five non immunosuppressed patients with biopsy proven pulmonary *M.tb* infection were analysed. The positive controls colon tumours (AMPK) from 10 patients and inflammed appendix (MMP-8). Negative controls were performed using the appropriate isotype control antibodies. Sections were immunostained for MMP-8 and phospho-AMPK alpha 1 and 2 (T172); neutrophil elastase with epitope retrieval performed by enzyme digestion using Bond Enzyme Pretreatment Kit. All antibodies were incubated for 15 minutes at room temperature. All immunohistochemistry was performed using the Leica Bond-III automated platform and associated ancillary reagents (all Leica Biosystems). The antibodies were detected using the Bond Polymer Refine Detection System and Bond DAB Enhancer according the manufacturer's instructions.

Statistical analyses

Data were analyzed using GraphPad Prism (version 5.04, GraphPad Software). Data are expressed as mean ± s.d. unless stated otherwise. All experiments are performed in biological triplicates on at least 2 separate occasions. Multiple intervention experiments are compared

with one-way ANOVA followed by Tukey's post-test correction, while continuous variables between 2 sets of data are assessed using two-tailed Mann-Whitney-U test. Spearman's rank correlation tests are used for correlation analyses. *P* values of less than 0.05 are taken as statistically significant.

Supporting Information

S1 Table. Demographic data of healthy controls and TB patients.
(DOCX)

S1 Fig. (A) TIMP-1 secretion is not increased with *M.tb* multiplicity of infection (MOI) at 4 hours. (B) TIMP-2 concentrations increase in a dose-dependent manner with *M.tb* MOI at 4 hours. (C) NF-kB inhibition suppresses neutrophil MMP-8 secretion driven by *M.tb* infection. Neutrophils were preincubated with p65 unit inhibitor Helenalin for 30 minutes and stimulated with *M.tb* MOI of 10 for 4 hours. (D and E) NF-kB inhibition suppresses neutrophil MMP-8 secretion driven by *M.tb* infection. Neutrophils were pre-incubated with caffeic acid phenethyl ester (CAPE) or SN50 for 30 minutes and stimulated with *M.tb* MOI of 10 for 4 hours. Bars represent mean ± s.d. of experiments performed in biological triplicates and is representative of at least 2 experiments. Analysis done by one-way ANOVA. ** $P<0.01$, *** $P<0.001$.
(TIF)

S2 Fig. NF-kB inhibition does not affect cell viability. Neutrophil viability of conditions for Fig 1D and 1E by FACS staining with Annexin V and live/dead dye. 50,000 events were gated. FACS plots representative of 2 donors.
(TIF)

S3 Fig. Necrotic centre of granuloma is positive for MMP-8. Biopsy proven *M.tb* infected human lung specimens were stained for MMP-8 and matched isotype control antibody.
(TIF)

S4 Fig. *M.tb* induces NETs. (A) Neutrophils were stimulated with *M.tb* MOI of 10 or 20nM PMA for 4 hours and NETs quantified using Picogreen QuantIT. All bars represent mean ± s.d. of experiments done in biological triplicates and are representative of a minimum of 2 independent experiments. (B and C) *M.tb* induced neutrophil extracellular traps are associated with MMP-8. Neutrophils were stimulated with PMA or infected with *M.tb* MOI 10 for 4 hours. DNAse was added into selected conditions. (D) Citrulline H3 is not associated with dead neutrophils. Neutrophils were either stimulated with PMA or lysed with Triton-X. 10μg of protein from cell-free supernatant were acetone precipitated and immunoblotted.
(TIF)

S5 Fig. Gelatinase degradation of respiratory secretions from healthy controls and TB patients. (**A**) TB patients have increased gelatinase activity in their induced sputum samples. (n = 11 both groups). **** $P<0.0001$. (**B**) Anti-MMP-9 neutralizing antibody at final concentration of 10 μg/ml does not decrease gelatinase activity in the induced sputum of TB patients (n = 11).
(TIF)

S6 Fig. Densitometric analysis from human protein kinase phosphoarray. Neutrophils were stimulated with CoMCont or CoMTB for 30 minutes. (A) Components of the MAP-kinase pathway. (B) Components of the STAT pathway. (C) Components of other signalling pathways. Protein kinase dots were normalized to control dots on each membrane. Bars represent

mean from arrays of 4 human donors.
(TIF)

S7 Fig. Neutrophil MMP secretion is independent of Akt/PI3 kinase and mTOR/p70S6K pathway. (A, D) Neutrophils were stimulated with CoMCont or CoMTB and lysed at specified time points. (B, C and E) Neutrophils were pre-incubated with Akt-inhibitor, LY 294002 or rapamycin prior to stimulation with CoMTB. P = NS. Bars represent mean ± s.d. of an experiment done in biological triplicates and is representative of a minimum of 2 independent experiments.
(TIF)

Acknowledgments

We are grateful to Jenny Paterson and Dr. Ian Teo for excellent technical assistance.

Author Contributions

Performed the experiments: CWMO SB PJP RCM TS. Analyzed the data: CWMO PTE LBT JCP JSF. Contributed reagents/materials/analysis tools: CUG MTTE VP RHG JCP. Wrote the paper: CWMO PTE JSF. Conceived the project: JSF. Designed the experiments: CWMO PTE JSF.

References

1. Eum SY, Kong JH, Hong MS, Lee YJ, Kim JH, Hwang SH, et al. Neutrophils are the predominant infected phagocytic cells in the airways of patients with active pulmonary TB. Chest. 2010 Jan; 137 (1):122–8. doi: 10.1378/chest.09-0903 PMID: 19749004
2. Nouailles G, Dorhoi A, Koch M, Zerrahn J, Weiner J, 3rd, Fae KC, et al. CXCL5-secreting pulmonary epithelial cells drive destructive neutrophilic inflammation in tuberculosis. J Clin Invest. 2014 Feb 10.
3. Harding MG, Zhang K, Conly J, Kubes P. Neutrophil Crawling in Capillaries; A Novel Immune Response to Staphylococcus aureus. PLoS Pathog. 2014 Oct; 10(10):e1004379. doi: 10.1371/journal.ppat.1004379 PMID: 25299673
4. Mantovani A, Cassatella MA, Costantini C, Jaillon S. Neutrophils in the activation and regulation of innate and adaptive immunity. Nat Rev Immunol. 2011 Aug; 11(8):519–31. doi: 10.1038/nri3024 PMID: 21785456
5. Parks WC, Wilson CL, Lopez-Boado YS. Matrix metalloproteinases as modulators of inflammation and innate immunity. Nat Rev Immunol. 2004 Aug; 4(8):617–29. PMID: 15286728
6. Nagase H, Visse R, Murphy G. Structure and function of matrix metalloproteinases and TIMPs. Cardiovasc Res. 2006 Feb 15; 69(3):562–73. PMID: 16405877
7. Ong CW, Elkington PT, Friedland JS. Tuberculosis, pulmonary cavitation, and matrix metalloproteinases. Am J Respir Crit Care Med. 2014 Jul 1; 190(1):9–18. doi: 10.1164/rccm.201311-2106PP PMID: 24713029
8. Volkman HE, Pozos TC, Zheng J, Davis JM, Rawls JF, Ramakrishnan L. Tuberculous granuloma induction via interaction of a bacterial secreted protein with host epithelium. Science. 2010 Jan 22; 327 (5964):466–9. doi: 10.1126/science.1179663 PMID: 20007864
9. Elkington P, Shiomi T, Breen R, Nuttall RK, Ugarte-Gil CA, Walker NF, et al. MMP-1 drives immunopathology in human tuberculosis and transgenic mice. J Clin Invest. 2011 May; 121(5):1827–33. doi: 10.1172/JCI45666 PMID: 21519144
10. Walker NF, Clark SO, Oni T, Andreu N, Tezera L, Singh S, et al. Doxycycline and HIV infection suppress tuberculosis-induced matrix metalloproteinases. Am J Respir Crit Care Med. 2012 May 1; 185 (9):989–97. doi: 10.1164/rccm.201110-1769OC PMID: 22345579
11. Price NM, Farrar J, Tran TT, Nguyen TH, Tran TH, Friedland JS. Identification of a matrix-degrading phenotype in human tuberculosis in vitro and in vivo. J Immunol. 2001 Mar 15; 166(6):4223–30. PMID: 11238675
12. Green JA, Tran CT, Farrar JJ, Nguyen MT, Nguyen PH, Dinh SX, et al. Dexamethasone, cerebrospinal fluid matrix metalloproteinase concentrations and clinical outcomes in tuberculous meningitis. PLoS One. 2009; 4(9):e7277. doi: 10.1371/journal.pone.0007277 PMID: 19789647

13. O'Neill LA, Hardie DG. Metabolism of inflammation limited by AMPK and pseudo-starvation. Nature. 2013 Jan 17; 493(7432):346–55. doi: 10.1038/nature11862 PMID: 23325217

14. Finlay D, Cantrell DA. Metabolism, migration and memory in cytotoxic T cells. Nat Rev Immunol. 2011 Feb; 11(2):109–17. doi: 10.1038/nri2888 PMID: 21233853

15. Chan O, Burke JD, Gao DF, Fish EN. The chemokine CCL5 regulates glucose uptake and AMP kinase signaling in activated T cells to facilitate chemotaxis. J Biol Chem. 2012 Aug 24; 287(35):29406–16. doi: 10.1074/jbc.M112.348946 PMID: 22782897

16. Pan H, Yan BS, Rojas M, Shebzukhov YV, Zhou H, Kobzik L, et al. Ipr1 gene mediates innate immunity to tuberculosis. Nature. 2005 Apr 7; 434(7034):767–72. PMID: 15815631

17. Calderon VE, Valbuena G, Goez Y, Judy BM, Huante MB, Sutjita P, et al. A humanized mouse model of tuberculosis. PLoS One. 2013; 8(5):e63331. doi: 10.1371/journal.pone.0063331 PMID: 23691024

18. Al Shammari B, Shiomi T, Tezera L, Bielecka MK, Workman V, Sathyamoorthy T, et al. The extracellular matrix regulates granuloma necrosis in tuberculosis. J Infect Dis. 2015 Feb 12.

19. Cooper AM, Dalton DK, Stewart TA, Griffin JP, Russell DG, Orme IM. Disseminated tuberculosis in interferon gamma gene-disrupted mice. J Exp Med. 1993 Dec 1; 178(6):2243–7. PMID: 8245795

20. Flynn JL, Chan J, Triebold KJ, Dalton DK, Stewart TA, Bloom BR. An essential role for interferon gamma in resistance to Mycobacterium tuberculosis infection. J Exp Med. 1993 Dec 1; 178(6):2249–54. PMID: 7504064

21. Mohan VP, Scanga CA, Yu K, Scott HM, Tanaka KE, Tsang E, et al. Effects of tumor necrosis factor alpha on host immune response in chronic persistent tuberculosis: possible role for limiting pathology. Infect Immun. 2001 Mar; 69(3):1847–55. PMID: 11179363

22. Davey MS, Tamassia N, Rossato M, Bazzoni F, Calzetti F, Bruderek K, et al. Failure to detect production of IL-10 by activated human neutrophils. Nat Immunol. 2011 Nov; 12(11):1017–8; author reply 8–20. doi: 10.1038/ni.2111 PMID: 22012430

23. Risso A. Leukocyte antimicrobial peptides: multifunctional effector molecules of innate immunity. J Leukoc Biol. 2000 Dec; 68(6):785–92. PMID: 11129645

24. Condliffe AM, Davidson K, Anderson KE, Ellson CD, Crabbe T, Okkenhaug K, et al. Sequential activation of class IB and class IA PI3K is important for the primed respiratory burst of human but not murine neutrophils. Blood. 2005 Aug 15; 106(4):1432–40. PMID: 15878979

25. Price B, Dennison C, Tschesche H, Elliott E. Neutrophil tissue inhibitor of matrix metalloproteinases-1 occurs in novel vesicles that do not fuse with the phagosome. J Biol Chem. 2000 Sep 8; 275 (36):28308–15. PMID: 10869345

26. Cuadrado E, Ortega L, Hernandez-Guillamon M, Penalba A, Fernandez-Cadenas I, Rosell A, et al. Tissue plasminogen activator (t-PA) promotes neutrophil degranulation and MMP-9 release. J Leukoc Biol. 2008 Jul; 84(1):207–14. doi: 10.1189/jlb.0907606 PMID: 18390930

27. Natarajan K, Singh S, Burke TR Jr., Grunberger D, Aggarwal BB. Caffeic acid phenethyl ester is a potent and specific inhibitor of activation of nuclear transcription factor NF-kappa B. Proc Natl Acad Sci U S A. 1996 Aug 20; 93(17):9090–5. PMID: 8799159

28. Ward C, Chilvers ER, Lawson MF, Pryde JG, Fujihara S, Farrow SN, et al. NF-kappaB activation is a critical regulator of human granulocyte apoptosis in vitro. J Biol Chem. 1999 Feb 12; 274(7):4309–18. PMID: 9933632

29. Kang DD, Lin Y, Moreno JR, Randall TD, Khader SA. Profiling early lung immune responses in the mouse model of tuberculosis. PLoS One. 2011; 6(1):e16161. doi: 10.1371/journal.pone.0016161 PMID: 21249199

30. Soehnlein O, Zernecke A, Eriksson EE, Rothfuchs AG, Pham CT, Herwald H, et al. Neutrophil secretion products pave the way for inflammatory monocytes. Blood. 2008 Aug 15; 112(4):1461–71. doi: 10.1182/blood-2008-02-139634 PMID: 18490516

31. Seyer JM, Hutcheson ET, Kang AH. Collagen polymorphism in idiopathic chronic pulmonary fibrosis. J Clin Invest. 1976 Jun; 57(6):1498–507. PMID: 777026

32. Gapski R, Hasturk H, Van Dyke TE, Oringer RJ, Wang S, Braun TM, et al. Systemic MMP inhibition for periodontal wound repair: results of a multi-centre randomized-controlled clinical trial. J Clin Periodontol. 2009 Feb; 36(2):149–56. doi: 10.1111/j.1600-051X.2008.01351.x PMID: 19207891

33. Ugarte-Gil CA, Elkington P, Gilman RH, Coronel J, Tezera LB, Bernabe-Ortiz A, et al. Induced Sputum MMP-1, -3 & -8 Concentrations during Treatment of Tuberculosis. PLoS One. 2013; 8(4):e61333. doi: 10.1371/journal.pone.0061333 PMID: 23613834

34. Neeli I, Radic M. Knotting the NETs: analyzing histone modifications in neutrophil extracellular traps. Arthritis Res Ther. 2012; 14(2):115. doi: 10.1186/ar3773 PMID: 22524286

35. Brill A, Fuchs TA, Savchenko AS, Thomas GM, Martinod K, De Meyer SF, et al. Neutrophil extracellular traps promote deep vein thrombosis in mice. J Thromb Haemost. 2012 Jan; 10(1):136–44. doi: 10.1111/j.1538-7836.2011.04544.x PMID: 22044575

36. Alfakry H, Sinisalo J, Paju S, Nieminen MS, Valtonen V, Tervahartiala T, et al. The association of serum neutrophil markers and acute coronary syndrome. Scand J Immunol. 2012 Aug; 76(2):181–7. doi: 10.1111/j.1365-3083.2012.02718.x PMID: 22537345

37. Carlson M, Raab Y, Seveus L, Xu S, Hallgren R, Venge P. Human neutrophil lipocalin is a unique marker of neutrophil inflammation in ulcerative colitis and proctitis. Gut. 2002 Apr; 50(4):501–6. PMID: 11889070

38. Ramos-DeSimone N, Moll UM, Quigley JP, French DL. Inhibition of matrix metalloproteinase 9 activation by a specific monoclonal antibody. Hybridoma. 1993 Aug; 12(4):349–63. PMID: 8244415

39. Berry MP, Graham CM, McNab FW, Xu Z, Bloch SA, Oni T, et al. An interferon-inducible neutrophil-driven blood transcriptional signature in human tuberculosis. Nature. 2010 Aug 19; 466(7309):973–7. doi: 10.1038/nature09247 PMID: 20725040

40. Danelishvili L, McGarvey J, Li YJ, Bermudez LE. Mycobacterium tuberculosis infection causes different levels of apoptosis and necrosis in human macrophages and alveolar epithelial cells. Cell Microbiol. 2003 Sep; 5(9):649–60. PMID: 12925134

41. Karim AF, Chandra P, Chopra A, Siddiqui Z, Bhaskar A, Singh A, et al. Express path analysis identifies a tyrosine kinase Src-centric network regulating divergent host responses to Mycobacterium tuberculosis infection. J Biol Chem. 2011 Nov 18; 286(46):40307–19. doi: 10.1074/jbc.M111.266239 PMID: 21953458

42. Hahn-Windgassen A, Nogueira V, Chen CC, Skeen JE, Sonenberg N, Hay N. Akt activates the mammalian target of rapamycin by regulating cellular ATP level and AMPK activity. J Biol Chem. 2005 Sep 16; 280(37):32081–9. PMID: 16027121

43. Zou MH, Hou XY, Shi CM, Kirkpatick S, Liu F, Goldman MH, et al. Activation of 5'-AMP-activated kinase is mediated through c-Src and phosphoinositide 3-kinase activity during hypoxia-reoxygenation of bovine aortic endothelial cells. Role of peroxynitrite. J Biol Chem. 2003 Sep 5; 278(36):34003–10. PMID: 12824177

44. Singh S, Saraiva L, Elkington PT, Friedland JS. Regulation of matrix metalloproteinase-1, -3, and -9 in Mycobacterium tuberculosis-dependent respiratory networks by the rapamycin-sensitive PI3K/p70S6K cascade. FASEB J. 2013 Oct 4.

45. Hardie DG, Ross FA, Hawley SA. AMPK: a nutrient and energy sensor that maintains energy homeostasis. Nat Rev Mol Cell Biol. 2012 Apr; 13(4):251–62. doi: 10.1038/nrm3311 PMID: 22436748

46. Kodiha M, Rassi JG, Brown CM, Stochaj U. Localization of AMP kinase is regulated by stress, cell density, and signaling through the MEK—>ERK1/2 pathway. Am J Physiol Cell Physiol. 2007 Nov; 293(5): C1427–36. PMID: 17728396

47. Arad M, Seidman CE, Seidman JG. AMP-activated protein kinase in the heart: role during health and disease. Circ Res. 2007 Mar 2; 100(4):474–88. PMID: 17332438

48. Scott JW, Hawley SA, Green KA, Anis M, Stewart G, Scullion GA, et al. CBS domains form energy-sensing modules whose binding of adenosine ligands is disrupted by disease mutations. J Clin Invest. 2004 Jan; 113(2):274–84. PMID: 14722619

49. Condos R, Rom WN, Liu YM, Schluger NW. Local immune responses correlate with presentation and outcome in tuberculosis. Am J Respir Crit Care Med. 1998 Mar; 157(3 Pt 1):729–35. PMID: 9517583

50. Sathyamoorthy T, Sandhu G, Tezera LB, Thomas R, Singhania A, Woelk CH, et al. Gender-dependent differences in plasma matrix metalloproteinase-8 elevated in pulmonary tuberculosis. PLoS One. 2015; 10(1):e0117605. doi: 10.1371/journal.pone.0117605 PMID: 25635689

51. Desvignes L, Ernst JD. Interferon-gamma-responsive nonhematopoietic cells regulate the immune response to Mycobacterium tuberculosis. Immunity. 2009 Dec 18; 31(6):974–85. doi: 10.1016/j.immuni.2009.10.007 PMID: 20064452

52. Nandi B, Behar SM. Regulation of neutrophils by interferon-gamma limits lung inflammation during tuberculosis infection. J Exp Med. 2011 Oct 24; 208(11):2251–62. doi: 10.1084/jem.20110919 PMID: 21967766

53. Kozakiewicz L, Chen Y, Xu J, Wang Y, Dunussi-Joannopoulos K, Ou Q, et al. B cells regulate neutrophilia during Mycobacterium tuberculosis infection and BCG vaccination by modulating the interleukin-17 response. PLoS Pathog. 2013; 9(7):e1003472. doi: 10.1371/journal.ppat.1003472 PMID: 23853593

54. Xu J, Zhang X, Pelayo R, Monestier M, Ammollo CT, Semeraro F, et al. Extracellular histones are major mediators of death in sepsis. Nat Med. 2009 Nov; 15(11):1318–21. doi: 10.1038/nm.2053 PMID: 19855397

55. Saffarzadeh M, Juenemann C, Queisser MA, Lochnit G, Barreto G, Galuska SP, et al. Neutrophil extracellular traps directly induce epithelial and endothelial cell death: a predominant role of histones. PLoS One. 2012; 7(2):e32366. doi: 10.1371/journal.pone.0032366 PMID: 22389696

56. Graham SA, Antonopoulos A, Hitchen PG, Haslam SM, Dell A, Drickamer K, et al. Identification of neutrophil granule glycoproteins as Lewis(x)-containing ligands cleared by the scavenger receptor C-type lectin. J Biol Chem. 2011 Jul 8; 286(27):24336–49. doi: 10.1074/jbc.M111.244772 PMID: 21561871

57. Segura-Valdez L, Pardo A, Gaxiola M, Uhal BD, Becerril C, Selman M. Upregulation of gelatinases A and B, collagenases 1 and 2, and increased parenchymal cell death in COPD. Chest. 2000 Mar; 117 (3):684–94. PMID: 10712992

58. Albaiceta GM, Gutierrez-Fernandez A, Garcia-Prieto E, Puente XS, Parra D, Astudillo A, et al. Absence or inhibition of matrix metalloproteinase-8 decreases ventilator-induced lung injury. Am J Respir Cell Mol Biol. 2010 Nov; 43(5):555–63. doi: 10.1165/rcmb.2009-0034OC PMID: 19995943

59. Guo L, Stripay JL, Zhang X, Collage RD, Hulver M, Carchman EH, et al. CaMKIalpha regulates AMP kinase-dependent, TORC-1-independent autophagy during lipopolysaccharide-induced acute lung neutrophilic inflammation. J Immunol. 2013 Apr 1; 190(7):3620–8. doi: 10.4049/jimmunol.1102975 PMID: 23447692

60. Hoogendijk AJ, Pinhancos SS, van der Poll T, Wieland CW. AMP-activated protein kinase activation by 5-aminoimidazole-4-carbox-amide-1-beta-D-ribofuranoside (AICAR) reduces lipoteichoic acid-induced lung inflammation. J Biol Chem. 2013 Mar 8; 288(10):7047–52. doi: 10.1074/jbc.M112.413138 PMID: 23322781

61. Wang S, Zhang C, Zhang M, Liang B, Zhu H, Lee J, et al. Activation of AMP-activated protein kinase alpha2 by nicotine instigates formation of abdominal aortic aneurysms in mice in vivo. Nat Med. 2012 Jun; 18(6):902–10. doi: 10.1038/nm.2711 PMID: 22561688

62. Mihaylova MM, Shaw RJ. The AMPK signalling pathway coordinates cell growth, autophagy and metabolism. Nat Cell Biol. 2011 Sep; 13(9):1016–23. doi: 10.1038/ncb2329 PMID: 21892142

63. Wejse C, Gustafson P, Nielsen J, Gomes VF, Aaby P, Andersen PL, et al. TBscore: Signs and symptoms from tuberculosis patients in a low-resource setting have predictive value and may be used to assess clinical course. Scand J Infect Dis. 2008; 40(2):111–20. PMID: 17852907